Introduction

Research Motivation

Large-scale surface inspection is widely demanded in manufacturing, infrastructure maintenance, and safety assurance. Large metal or composite structures like aircraft skins require regular inspection to detect defects that may limit performance or safety. GelBelt [1], a vision-based tactile sensor for continuous sensing of large surfaces, can maintain the reconstruction accuracy of the dot product of the estimated and reference surface normal maps above 0.97. By taking GelBelt and making it a mobile robot that can autonomously traverse large surfaces, we are creating a complete inspection solution that can collect high-quality data with minimal human effort.

Literature Review

Tactile sensing can provide high-resolution geometry and contact forces, which are essential for detecting small surface defects and monitoring contact conditions, something that vision-only inspection often cannot achieve. Vision-based tactile sensors (VBTS), such as GelSight [2], use a deformable elastomer coated with a reflective membrane and illuminated by colored lights. An internal camera records the deformation of this surface, producing high-resolution 3D geometry and local force measurements. GelSight enables detailed geometry reconstruction and force sensing, but its sensing area is small, and the elastomer pad is rigidly attached to the sensor body, which limits continuous scanning over large surfaces. Early optical tactile pads [3], based on deformable elastomer and optical fiber, offered similar high spatial resolution but suffered from comparable sensing-area limitations, making sliding over surfaces challenging. Nanogenerator-based sensors [4] generate electrical pulses from sliding motion over textured surfaces, allowing recognition of roughness and texture, but they are generally suited for small-scale contact and less effective on highly curved surfaces.

GelBelt [1] is specifically designed for continuous sensing of large surfaces. Instead of a fixed elastomer pad, GelBelt uses an elastomeric belt that rolls over two wheels, which enables continuous scanning while maintaining a large scanning area in each frame and high geometric resolution. The GelBelt demonstrated accurate surface normal reconstruction and defect detection, with a speed of up to 45mm/s. For surface scanning, this device was operated by a robot arm and, therefore, was limited to surfaces reachable by the arm.

Climbing robots reach surfaces that a robot arm fails to, such as surfaces that are large or physically hard to access, in addition to surfaces that are vertical or inverted. We looked at various climbing robots to begin our design. A gecko-inspired climbing robot [5] uses adaptive active suction modules, each made of three small suction pads arranged so they can rotate

independently, which maintain adhesion even on uneven surfaces. This robot shows us that active suction can be very effective and powerful for curved and uneven surfaces; however, this method of locomotion would interrupt sensing continuity. There are also wall-climbing robots that developed a passive suction climbing module [6], which used torsion springs to attach the suction cups and used a wire to peel off and detach. This robot was further iterated on with a tracked belt and a tail [7] to provide reaction forces that helped the module stick to the wall. The design seemed to work well for adhering and climbing smooth surfaces, but there was too much vibration, which caused the robot to "snake" off course, and there was no steering mechanism.

We also evaluated alternative adhesion technologies [8]. Gecko-inspired dry adhesives were initially considered, but commercial solutions such as Gecko Materials' adhesive pads were impractically expensive given our constraints. Magnets, electrostatic adhesion, and grasping grippers also appeared less feasible or suitable due to aircraft skin material, curvature, required contact continuity, and safety constraints.

Aerial robots are capable of rapidly reaching remote or complex areas. CityFlyer system [9] uses quadrotor robots with RGB-D cameras to inspect concrete defects, generate 3D mapping, and shows that aerial robots can be used in automated visual inspection and reconstruct dense 3D models, but it lacks tactile information and only relies on visual information. Aerial robots that fly near surfaces, particularly under an overhanging surface, experience an increase in thrust and a reduction in power consumption, which is observed as the ceiling effect [10]. A quadrotor near a wall has also shown suction forces generated by the wall-proximity effect [11] and developed model-predictive controls to prevent colliding near vertical surfaces. These results demonstrate the potential of combining aerial systems with near-surface operations, but they pose challenges in providing continuous contact along the surface.

Design Objectives

To extend the sensing capability to vertical or inverted surfaces, we integrated the GelBelt into a mobile robot with suction-based adhesion. This robot uses an array of suction cups to attach to the surface being scanned. The control system is designed to maintain a minimum of 10 N of force into the surface, which is necessary for accurate tactile sensing, while also supporting the weight of the GelBelt and vacuum modules totaling approximately 25 N. Additionally, Gelbelt needs to be in continuous and even contact with the target surface for consistent mapping. The robot is designed to conduct full-surface traversal across all orientations, without damaging the surface, and while minimizing energy consumption. Finally, we would like the system to be robust to rivets, seams, paint variation, and dust, as would be found on the wing of an aircraft.

Semester Project Objectives

We first focused on feasibility tests on our adhesion concepts and selected one approach for further development and prototyping. Since we initially proposed two concepts, suction cups

and a quadrotor, we evaluated each to determine which was the most optimal to pursue moving forward. After down-selection, we focused on component selection and on fabricating a suspension system and vacuum modules, which formed our primary engineering goals for the semester.

Progress

Adhesion Selection

We began by evaluating two primary concepts for the system's climbing and adhesion mechanism: suction cups and a quadrotor-assisted platform. Early-stage consideration focused on actuation feasibility, controllability, power consumption, and the ability to maintain stable contact across varied aircraft surface geometries.

Suction-Cup Based Testing

To assess the feasibility of suction-based adhesion, we considered the required number of suction cups, the per-cup holding strength, the net force generated in both the normal and shear directions, the surface roughness of the target aircraft skin, and material properties of each suction cup, such as softness, stiffness, and compliance.

To measure adhesion strength (maximum Fz, maximum shear, and performance on various materials), we designed an experiment that mounted a suction cup to a force–torque sensor and allowed it to move up and down a linear rail. The suction cup was pressed onto an acrylic platform at various levels of normal force, and the corresponding pulling Fz force was recorded. The acrylic sheet was mounted on an XY stage, which we moved laterally to measure the maximum shear force before detachment.

After identifying the suction cup that produced the highest adhesion force, we also tested it on curved surfaces, surfaces with different levels of roughness, and its active suction capabilities.

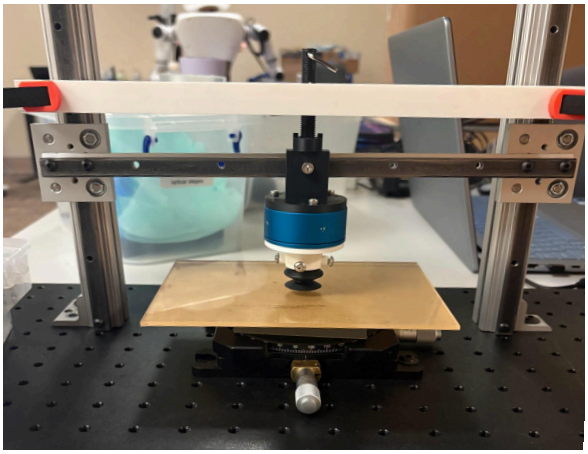

Figure 1. Suction-Cup Testbed Setup. There are 2 aluminum profiles on either side, which the linear rail rides. 3D printed parts connect the rail to the FT sensor, which has another mount to screw in the suction cups. There is a screw attached to a static block at the top so that the normal force can be controlled.

We began testing using Buna-N rubber (5427A106), Vinyl Plastic (7275A34), and Plastic (65825A3) material suction cups. Additionally, both the rubber and vinyl plastic cups had bellows (which allow them to conform to rougher surfaces) and were designed for active suction. We began by testing the max pulling force on acrylic.

Material	Pressing (Normal) Force (N)	Pulling Force (N)
Plastic	7	26.78
Buna-N Rubber	6	10.21
Buna-N rubber	7	10.85
Buna-N rubber	8	10.85
Buna-N rubber	9	9.86
Vinyl Plastic	6	25.63
Vinyl Plastic	7	30.36
Vinyl Plastic	8	29.33
Vinyl Plastic	9	21.70

Table 1. Normal Force Results

Vinyl plastic showed the best holding strength, so we moved on to shear, curved-surface, and active-suction testing in the XY plane, a curved aluminum profile, and a simple vacuum pump.

Shear testing was especially important because the robot will be moving vertically upward, meaning the suction cups must resist lateral slip during climbing. The curved aluminum profile was chosen because it closely resembles the curvature of an aircraft wing, allowing us to evaluate performance on a realistic aerospace surface. We also tested active suction to ensure robustness when moving across rivets, gaps, and other surface nonconformities.

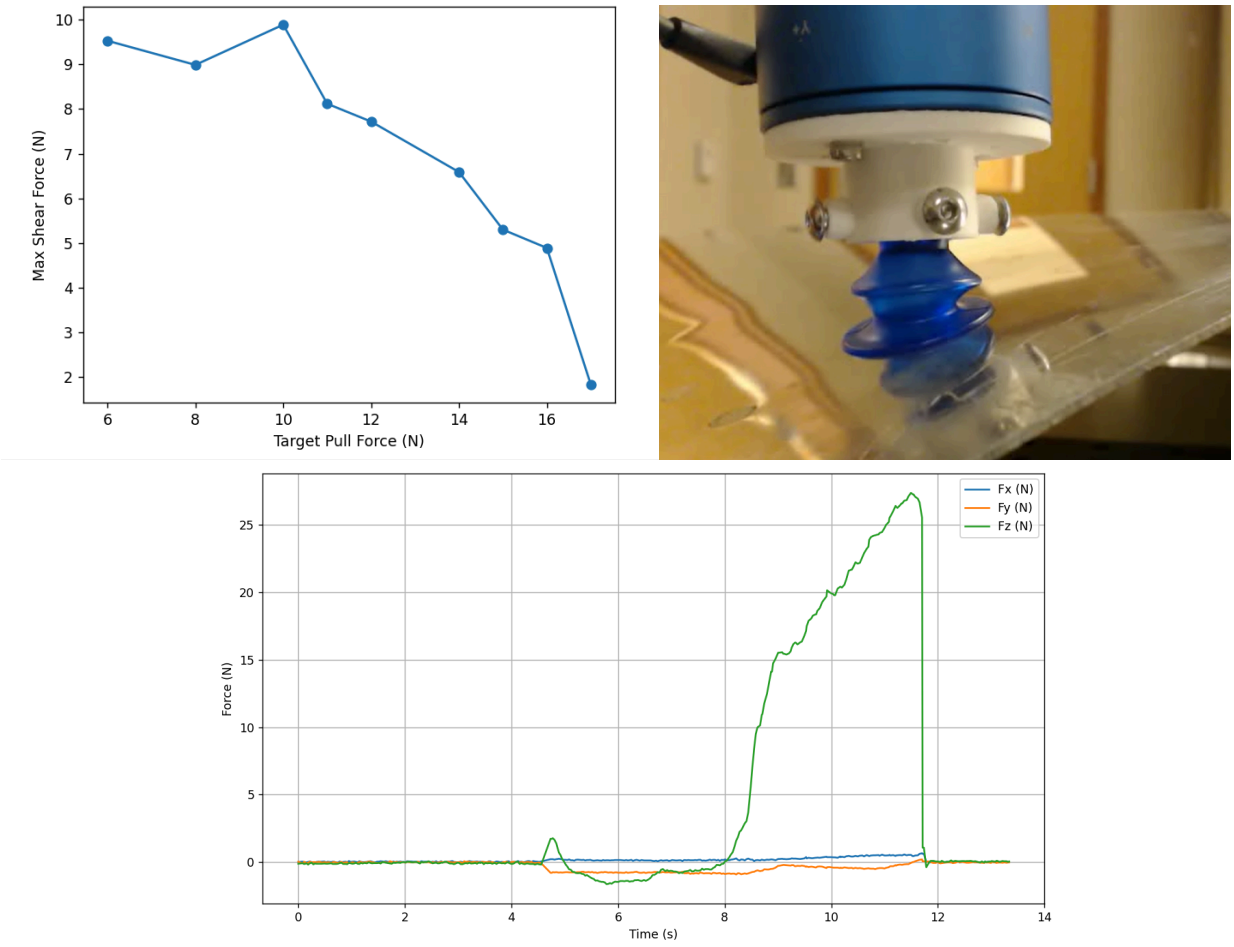

Figure 2. Continued testing Results (Shear, Curved, Active). The top left plot shows the shear and Fz forces plotted together, note that the cup peforms best before we reach 12N of force because the cup begins to leak after. The bottom plot shows our peak force using active suction which was >25N.

The single vinyl plastic cup was able to generate >9 N in shear, which exceeds our requirement since we would only need three cups to hold the weight of the system. It was also able to continue generating >20 N on the curved aluminum surface, which is our target. In shear testing, the active suction performed 2x better than passive suction, while the other metrics were relatively similar across materials. Another benefit is that we do not need to worry about pressing force because the cup can adhere on its own. The cup was also tested on curved and rougher surfaces, such as the textured backing on the acrylic sheet, and was still able to generate >20 N

of pulling force. Based on these results, we decided to move forward with the vinyl plastic suction cup. Based on the length of the GelBelt and the need for continuous locomotion, we are able to fit four suction cups in contact with the surface at a time. This provides redundancy in the system in case any of the suction cups fail.

Propeller and Motor Thrust Testing

The motor thrust experiments were held to determine whether a quadrotor configuration using Vertiq 23-06 motors could meet the system requirement, and to find how the ceiling effect would influence thrust and energy consumption when the propeller and the surface have a small distance. Our system requires at least 25 N of available thrust, approximately 15 N for the weight of the system, and 10 N to press the sensor into the surface.

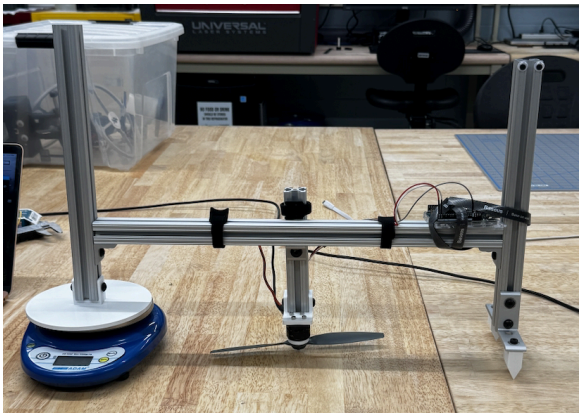

Figure 3. Thrust Test Setup. Vertiq 23-06 motor with a 21 cm propeller mounted at the center of a pivoting aluminum beam setup. The left support is on a digital scale to measure force, and the wooden table below serves as the ceiling surface.

Figure 3 shows the thrust test setup. A Vertiq 23-06 motor was attached to a horizontal aluminum beam, which pivoted about a joint above a digital scale. The propeller pointed downward toward a wooden table that acted as a “ceiling.” The distance between the propeller and the wooden table was adjustable along the beam, and the motor was mounted in the middle of the horizontal aluminum beam. For this experiment, we used an APC 6x3R propeller with a constant motor speed. The propeller to ceiling distance was varied from 0.5 cm to 5 cm, and thrust was recorded at each distance. The goal of this experiment was to understand how operating close to a surface would change the effective thrust, since a quadcopter inspecting an inverted surface would hover beneath the surface.

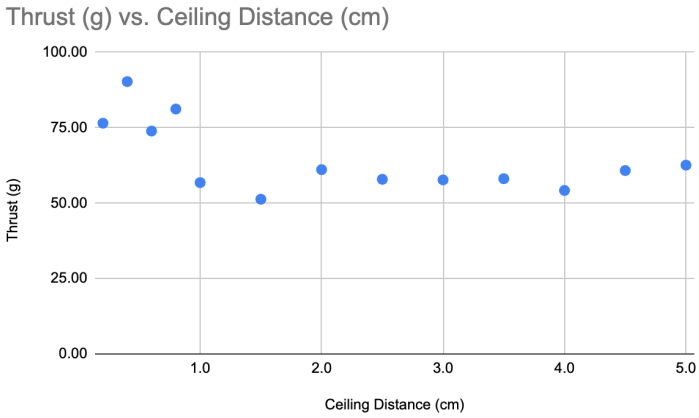

Figure 4. A chart showing the relationship between the thrust motor generated and the distance from the ceiling. The ceiling effect is shown when the ceiling distance is less than 1 cm.

Figure 4 shows that the ceiling effect is prominent when the propeller-to-ceiling distance is less than 1 cm. In this experiment, the motor angular speed, the dimension of the propeller, and the voltage from the power supply were kept constant.

Propeller	Status	Velocity (rad/s)	Temperature	Current (A)	Voltage (V)	Thrust (g)	Force (N)
6 x 3R	Start	1925.14	63.33	8.54	21.4	322	6.3
	2 min	1790.45	75.91	6.28	22.4	270	5.3
	5 min	1778.45	76.76	5.88	23.2	265	5.2
5 x 3E	Start	2789.38	46.7	10.41	23.2	282	5.5
	2 min	2720.90	69.2	9.45	23.2	265	5.2
	5 min	2727.65	69.12	9.46	23.2	266	5.2

Table 2. Result of the motor thrust test without the ceiling effect

A maximum continuous thrust test with a propeller distance of 1.5 cm from the ceiling was held to determine whether the motor could provide the required 25 N of thrust for our application. Based on the manufacturer's thrust data for the Vertiq 23-06, we selected two commercially available APC propellers that were predicted to be near the motor's maximum thrust for our operating voltage. For each propeller, the propeller-ceiling distance was fixed at 1.5 cm, and the motor ran continuously for 5 minutes at a high speed. During each run, we recorded velocity, current, voltage, temperature, and thrust at the start, after 2 minutes, and after 5 minutes, which are shown in Table 2. Both propellers produced a continuous thrust of approximately 5.2 N at around 2700 rad/s, with modest heating of the motor but no significant drop in angular velocity over time.

Final Decision

Ultimately, we decided to move forward with active suction as our form of adhesion to surfaces. The results indicate that, even in favorable conditions and with propellers chosen near the

motor's performance limit, a single Vertiq 23-06 motor can generate only about 5 N of continuous thrust. A quadcopter would therefore provide around 20 N total thrust, which is insufficient for our required 25 N. In contrast, suction-cup experiments showed that our selected cups can provide attachment forces above 20 N per cup with lower power consumption and without relying on aerodynamic effects. Based on this comparison, we concluded that a propeller-based system would not meet our force requirements. Because of the better shear performance and added robustness, we decided to use active suction, which requires a small vacuum pump connected to each individual suction cup. Moving forward, this introduced several new considerations: the vacuum pump now had to interface with each suction cup through a rotary joint, a junction, and a pneumatic switch. In addition, we needed to develop a suspension system to evenly distribute force and press the GelBelt with approximately 10 N into the surface to generate proper sensor readings.

Connection Design

We use belts of suction cups to keep the GelBelt pressed against the surface while the robot moves. All cups on a belt share a single vacuum pump, but we need to individually control which cups are active so that only those near the sensing surface connect to the vacuum while cups facing away are blocked. This individual control improves adhesion and makes it easier to detach the belt from the surface. To satisfy these requirements, we designed a compact per-cup pneumatic valve and a small junction to distribute vacuum from one pump to multiple cups.

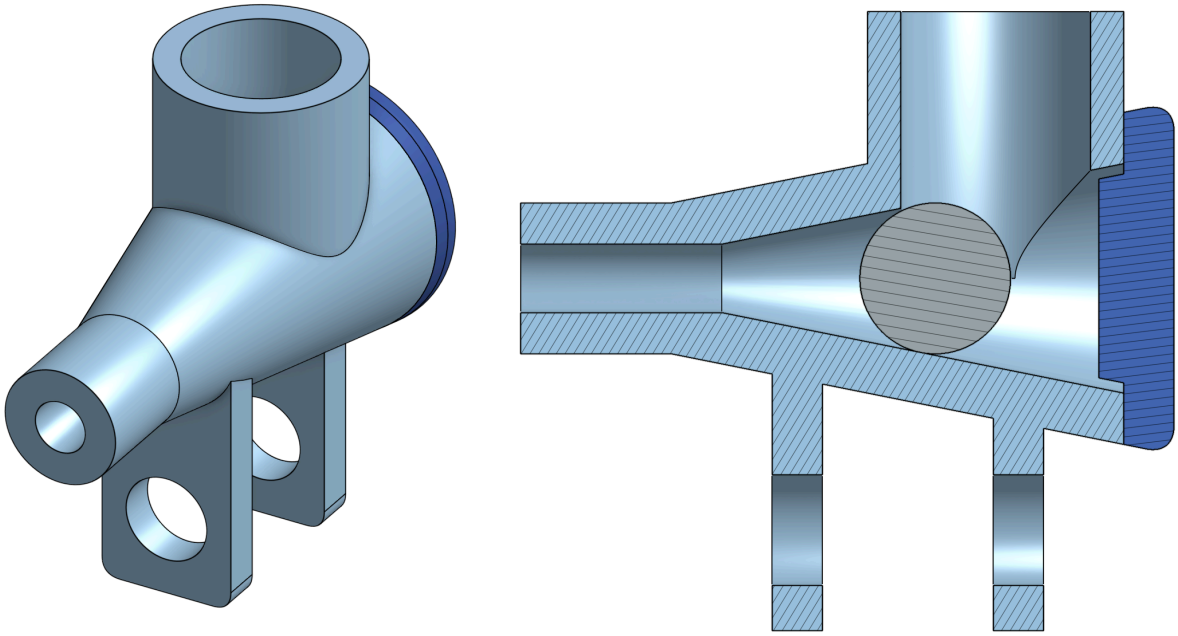

Figure 5. Pneumatic Valve and Its Cross-section

Figure 5 shows the initial per-cup pneumatic valve and its cross-section. The pneumatic valve is a small ball switch that lets one pump line control a single suction cup. The left port connects to

the vacuum pump, and the top port goes to the cup. When closed, a steel ball seats against the internal surface to block flow from the pump. To open the valve, an external magnet placed near the blue cap pulls the ball off, so the vacuum reaches the cup. For a reliable seal, the inner surface should have a soft elastomer so the ball seals on a soft surface rather than printed PLA. During testing, we observed two main issues. The ball did not always generate a reliable seal because the printed surface and contact area were small, which caused leakage. Once the ball was pulled tightly into the seat by vacuum, it was difficult to detach using an external magnet alone.

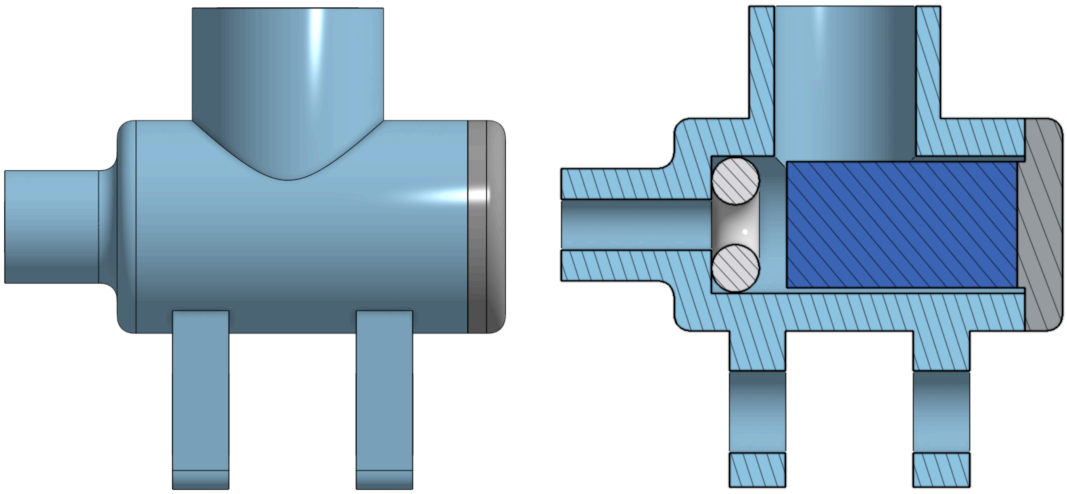

Figure 6. Pneumatic Valve with Magnet

To address these problems, we developed a second version of the valve, shown in Figure 6. This version uses the same mechanism, but has a magnet instead of a steel ball. Soft elastomer to ensure air seal was replaced with a silicone o-ring to make the fabrication process simpler, and the magnet inside will allow a stronger push and pull force against the o-ring when controlled by an external magnet, which makes the sealing and release more controllable than in the steel ball version.

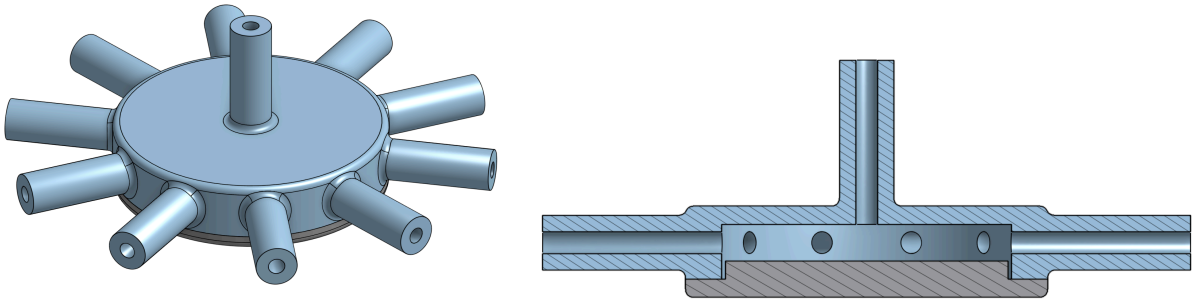

Figure 7. 10-port Junction and Its Cross-section

Figure 7 shows a 10-port junction that is made to share one vacuum pump among a number of suction cups. The top port is the inlet from the pump, and the ten ports on the side connect to individual cups (or the pneumatic valves). It simply distributes one supply to multiple ports.

Normal Force Compensation System

Maintaining a consistent normal force is necessary for the GelBelt to generate accurate measurements. Uneven force can lead to poor contact between the elastomeric belt and the surface, resulting in distorted or incomplete geometry and force readings. The normal force compensation system was designed to generate the >10 N force required to press the GelBelt into the surface. Suspension is necessary to both lift the climbing modules and push the GelBelt downward, while evenly distributing the GelBelt's weight across all suction cups in contact with the surface. Additionally, the system should provide sufficient compliance to absorb variations in surface height without detaching suction cups or overloading the mechanism.

System Modeling

We use springs and a selected suction cup's elastic model to design the entire suspension system. The elastic model of the suction cup was found by measuring deformation vs. force from our testing.

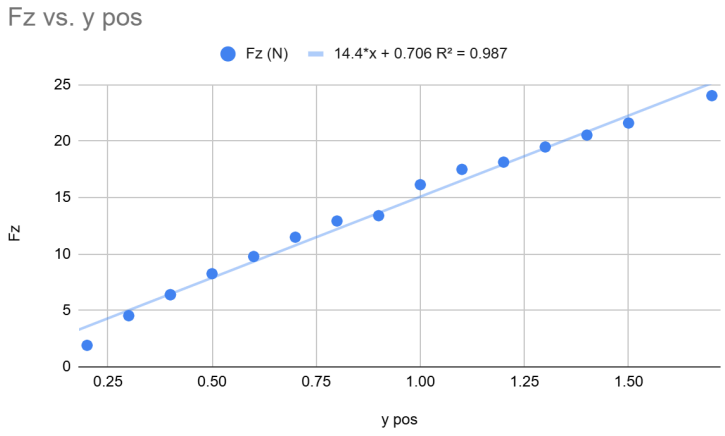

Figure 8. Suction Cup Elastic Model

We then developed force relationships to analyze the suspension.

```
# Core Force Relationships
F_cup  = F_weight + F_spring
k_cup * d_cup = F_weight + k_spring * (d_offset - d_cup)

# Offset Relationships
```

```
d_off = d_spring + d_cup = (1+r)*d_cup
# unknowns are k_spring and d_offset

# Assumptions
# Each suction cup behaves as a linear spring
# Suspension springs act in parallel to distribute force evenly
# Total system weight is shared among all cups in contact
F_weight = 20          # N
F_cup = 30       # N total
F_push = 10       # N required to push in gelbelt
k_cup = 14.4 * 8 # N/cm (all cups together)
d_suctionMax = 1.4  # cm

# Constraints
d_cup < d_suctionMax
K_spring >= F_gelbelt / d_suction / 4    # spring constant per corner
```

Ultimately, the offset was a design choice as there is a broad range of k-value - offset combinations that were feasible, so it came down to design choices to finalize the strength of the spring and offset. After referencing what was available, we found that a k = 5.248 lbs./in. (9.19 N/cm) spring would need an offset of around 1.4cm, which is closer to our upper bound. We also thought that it is better to keep the offset lower so that we can keep the overall system size/height smaller. As we get close to our lower bound (0.26cm), the K value goes up significantly > 50 N/cm, and a high k value is more difficult to work with. Around 1.5 cm is a reasonable offset and leaves room for error.

Suspension and Suction System Testing

To evaluate the suspension and suction systems under realistic loading, we built a test prototype that lacks the drive belts for motion but allows measurement of forces and evaluation of GelBelt image quality. We tested the system at a 2.116 kg system mass, which approximates the expected mass of the final robot, by adding weights to the module. This prototype allowed us to verify GelBelt image quality on flat, curved, and inverted surfaces in aluminum and acrylic.

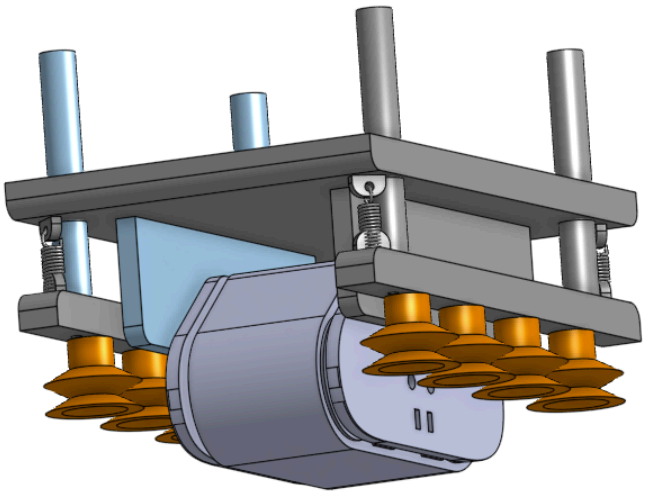

Figure 9. Suspension module CAD

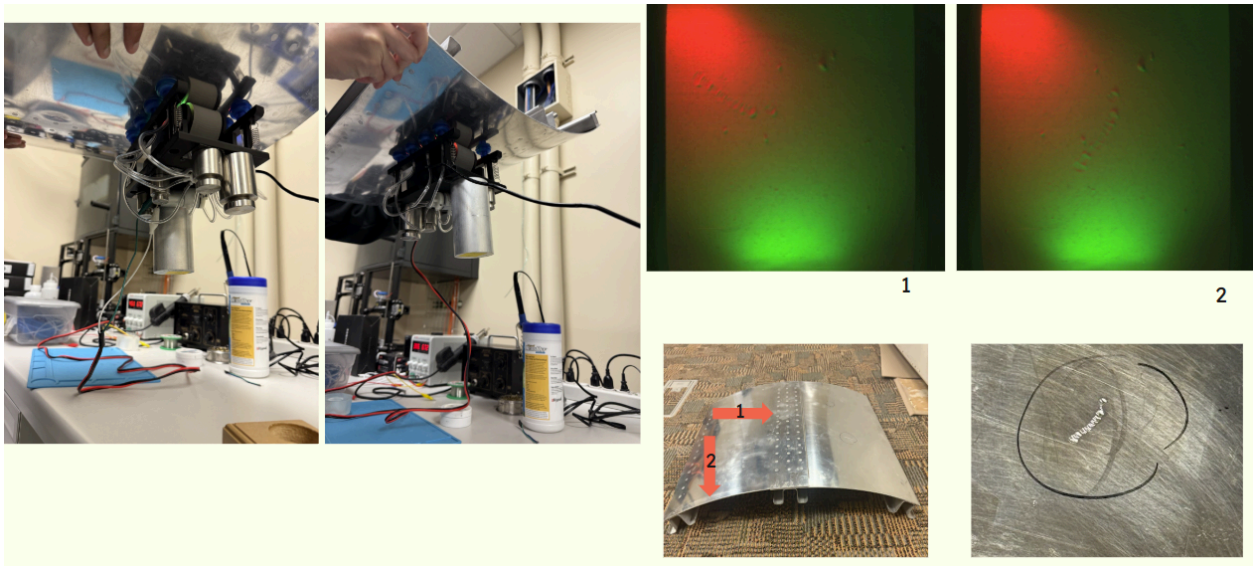

Figure 10. Curved Surface Test. The system module is attached to a curved aluminum surface in vertical (1) and horizontal (2) directions (bottom right). The module is attached to a curved aluminum profile (left), GelBelt images of the same region (top right) shows welded seams, and the aluminum surface was scanned on its weld defects (bottom right). The sensor clearly shows the defect while suction cups maintain stable contact with the curved surface.

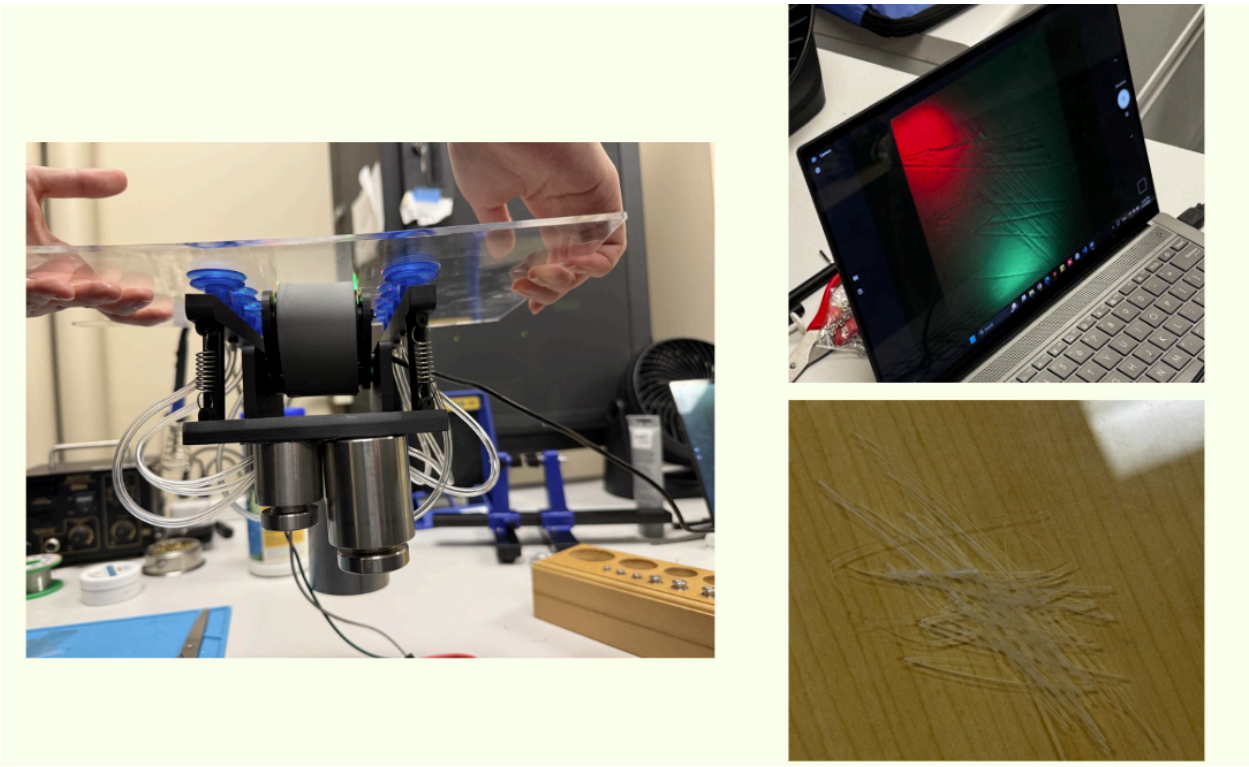

Figure 11. Inverted Test. The module is attached to the underside of the acrylic plate (left), live GelBelt image during the test is shown on the top right, and the picture of scratches on the acrylic surface is shown on the bottom right. The sensor clearly shows the scratch defects while the suction cups maintain table contact in the inverted orientation.

Figures 10 and 11 demonstrate that the suspension and suction modules with K = 9.19 N / cm with a 1.5 cm offset can maintain good GelBelt contact on both curved and inverted surfaces with clear sensor readings. In Figure 10, the module was attached to a curved aluminum surface in two directions, and gelbelt images of the contact region clearly showed the weld lines. This indicates that the suspension and suction systems provide enough force to follow the curvature while still maintaining normal force for reliable reconstruction. In Figure 11, the module was mounted under an acrylic plate, and the GelBelt images again showed the scratch defects on the acrylic. Additionally, the suction module was able to stick to the wall of the room with a rougher surface and detect the surface texture.

Conclusion

The primary goal of this semester was to evaluate the feasibility of different adhesion and actuation methods, down-select a final approach, and begin developing the key mechanical and pneumatic subsystems required for GelBelt locomotion. Through testing of suction cups, propeller thrust, suspension behavior, and surface interaction, we were able to compare our design options and choose the most viable path forward.

With adhesion and suspension validated, the project is positioned to begin locomotion development next semester. Future work will focus on belt actuation, suction-cup switching mechanisms, steering, and full-surface traversal. The progress made this term establishes a foundation for turning GelBelt into a fully mobile inspection platform.

References

[1] M. A. Mirzaee, H.-J. Huang, and W. Yuan, “GelBelt: A Vision-Based Tactile Sensor for Continuous Sensing of Large Surfaces,” *IEEE Robotics and Automation Letters*, vol. 10, no. 2, pp. 2016–2023, Feb. 2025. doi: 10.1109/LRA.2025.3527306.

[2] W. Yuan, S. Dong, and E. H. Adelson, “GelSight: High-Resolution Robot Tactile Sensors for Estimating Geometry and Force,” *Sensors*, vol. 17, no. 12, p. 2762, 2017. doi: 10.3390/s17122762.

[3] J. L. Schneiter and T. B. Sheridan, “An optical tactile sensor for manipulators,” *Robotics and Computer-Integrated Manufacturing*, vol. 1, no. 1, pp. 65–71, 1984. doi: 10.1016/0736-5845(84)90081-4.

[4] Z. Liao, et al., “A Tactile Sensor Translating Texture and Sliding Motion Information into Electrical Pulses,” *Nanoscale*, The Royal Society of Chemistry, May 18, 2015. Available: https://pubs.rsc.org/en/content/articlelanding/2015/nr/c5nr01509j

[5] C. Menon, M. Murphy, and M. Sitti, “Gecko Inspired Surface Climbing Robots,” in *Proc. 2004 IEEE International Conference on Robotics and Biomimetics*, Shenyang, China, 2004, pp. 431–436. doi: 10.1109/ROBIO.2004.1521817.

[6] J. Guo, G. Li, and N. Xi, “Design of a Wall-Climbing Robot With Passive Suction Cups,” in *2017 IEEE International Conference on Robotics and Biomimetics (ROBIO)*, 2017, pp. 1180–1185. doi: 10.1109/ROBIO.2017.8324560.

[7] D. Ge, Y. Tang, S. Ma, T. Matsuno, and C. Ren, “A Pressing Attachment Approach for a Wall-Climbing Robot Utilizing Passive Suction Cups,” *Robotics*, vol. 9, no. 2, p. 26, 2020. doi: 10.3390/robotics9020026.

[8] S. Sikdar, M. H. Rahman, A. Siddaiah, and P. L. Menezes, “Gecko-Inspired Adhesive Mechanisms and Adhesives for Robots — A Review,” *Robotics*, vol. 11, no. 6, p. 143, 2022. doi: 10.3390/robotics11060143.

[9] L. Yang, B. Li, W. Li, H. Brand, B. Jiang, and J. Xiao, “Concrete defects inspection and 3D mapping using CityFlyer quadrotor robot,” *IEEE/CAA Journal of Automatica Sinica*, vol. 7, no. 4, pp. 991–1002, Jul. 2020. doi: 10.1109/JAS.2020.1003234.

[10] Y. H. Hsiao and P. Chirarattananon, “Ceiling Effects for Surface Locomotion of Small Rotorcraft,” in *2018 IEEE/RSJ International Conference on Intelligent Robots and Systems (IROS)*, Madrid, Spain, 2018, pp. 6214–6219. doi: 10.1109/IROS.2018.8593726.

[11] P. Yang, W. Wen, R. Yang, Y. Chen, and C. C. Tsang, “Wall Inspector: Quadrotor Control in Wall-proximity Through Model Compensation,” *arXiv*, 2025. doi: 10.48550/arXiv.2509.21496.

Appendix

Project Materials and Documentation

All of our project materials are stored in boxes in the RoboTouch lab, and the documentation is in our Google Drive (NovelMobileRobotsLab > Projects > Mobile Gelbelt) for reports and presentation files, and in Box (NovelMobileRobotsLab > Projects > Mobile Gelbelt) for experiment results.

Current Work

We are currently developing the active suspension system and fabricating the pneumatic switches. The next major step will be achieving forward and backward locomotion, which requires designing the pulley, belt, and drive system. Our plan is to use a Dynamixel XC330-M288-T to drive a timing belt with ten suction cups attached to it.

Motor Considerations:
The motor has a stall torque at 5 V = 0.93 N·m
Target translational speed = 4 cm/s.
Revs needed = (4 cm/s) / (10 cm/rev) = 0.4 rev/s = 24 rev/min.
This rev speed (24 RPM) is low and within the motor's usable-speed range at 0.5 N·m.

Climb power estimate (worst case, going up the wall)
system mass = 2 kg
vertical speed = 4 cm/s = 0.04 m/s.
Power to lift = m * g * v = 2 * 10 * 0.04 = 0.8 W.
24 RPM = 0.4 rev/s, $\omega = 0.4 * 2\pi \approx 2.51$ rad/s.

Required torque (neglecting suction detachment forces and friction):
$T = \text{Power} / \omega = 0.8 / 2.51 \approx 0.32$ N·m. If we aim for ~ 0.5 N.m usable torque out of the motor, we have lots of clearance.

Bill of Materials

Item	Vendor	Part Number	Cost	Qty	Total	Notes
Suction cup prototype						
Uxcell 20mm/0.8 Inch PVC Suction Cups Sucker Pads Without Hooks for Home Kitchen Hanging, Clear 10 Pack	Walmart	9378504172	$7.490	1	$7.49	uxcell s24072600wm1496

Uxcell 0.8/1.2/1.8 Inch PVC Suction Cups Sucker Pads Without Hooks for Home Kitchen Hanging, Clear 30 Pack	Walmart	9391362713	$9.440	1	$9.44	uxcell s24072700wm0108
Vacuum Cup: Height -Adjustable, Push-on, Single Bellow, 1.09" Diameter, 0.8" Height	McMaster-Carr	7275A23	$11.34	1	$11.34	Active suction cup for testing
Vacuum Cup: Height -Adjusting, Push-on, Single Bellow, 0.93" Cup Diameter	McMaster-Carr	5427A106	$4.95	1	$4.95	Buna-N rubber material active suction cup for testing
Vacuum Cup: Push-on, 1" Cup Diameter, 0.340" Cup Height	McMaster-Carr	7275A34	$10.09	1	$10.09	Vinyl Plastic but no bellows
Suction-Cup Hooks: 1-1/8" Wide x 1-1/8" High x 1/2" Deep Overall	McMaster-Carr	65825A3	$11.64	1	$11.64	Has hooks(we can remove), pack of 25 is the minimum
Vacuum Cup: Height -Adjustable, Push-on, Single Bellow, 1.09" Diameter, 0.8" Height	McMaster-Carr	7275A23	$11.340	8	$90.72	
Corrosion-Resistant Extension Spring with Loop Ends 302 Stainless Steel, 0.875" Long, 0.240" OD, 0.031" Wire Diameter	McMaster-Carr	7749N108	$19.670	1	$19.67	Length: 0.875", k= 8.247 lbs./in. (14.45 N/cm)
Corrosion-Resistant Extension Spring with Loop Ends302 Stainless Steel, 0.875" Long, 0.360" OD, 0.031" Wire Diameter	McMaster-Carr	7749N09	$18.170	1	$18.17	Length: 0.875", k= 5.248 lbs./in. (9.19 N/cm)
Corrosion-Resistant 3003 Aluminum Tube Telescoping, 0.014" Wall Thickness, 1/8" OD, 1 Foot Long	McMaster-Carr	7237K14	$2.370	4	$9.48	Connection from suction cups to pneumatic tubing
L Series Timing Belt, Trade No. 367L050	McMaster-Carr	6484K156	$22.110	1	$21.11	For driving and suction cup attachment, will cut this belt to size, min length of each tread should be -15in for 10 suction cups
Neodymium Magnet with Adhesive on North Pole, 0.055" Thick, 1/2" Wide	McMaster-Carr	7048T75	$3.860	13	$50.18	Magnet for vacuum control through pneumatic valve
Neodymium Magnet with Adhesive on South Pole, 0.055" Thick, 1/2" Wide	McMaster-Carr	7048T74	$3.860	4	$15.44	Magnet for vacuum control through pneumatic valve
QSRL-M5-4	DigiKey	QSRL-M5-4	$18.500	2	$37.00	Pneumatic rotary joint to allow tubing to rotate with

						suction cups
Micro DC Worm Gear Motor w/ Encoder - 3V 18RPM	RobotShop	1220WG-N20VA-603-EN 3V	$15.700	1	$15.70	Active suspension motor, worm gear for locking position
High-Temperature High-Purity Silicone O-Rings 1/32 Fractional Width, Dash Number 001	McMaster-Carr	9396K101	$9.050	1	$9.05	Air seal in pneumatic valve (to allow magnetic ball to close valve)
High-Temperature High-Purity Silicone O-Rings 1/16 Fractional Width, Dash Number 005	McMaster-Carr	9396K63	$6.550	1	$6.55	Air seal in pneumatic valve, bigger size
Vacuum Cup: Height -Adjustable, Push-on, Single Bellow, 1.09" Diameter, 0.8" Height	McMaster-Carr	7275A23	$11.340	8	$90.72	
Brass Tapered Heat-Set Inserts for Plastic	McMaster-Carr	93365A201	$10.620	1	$10.62	Assembly/fastening parts together
Quadrotor prototype						
T-Slotted Framing 1/2 ft: T-Slotted Framing, Single Four Slot Rail, Silver, 1" High x 1" Wide, Solid, 1/2 ft	McMaster-Carr	47065T101-47065T553	$6.060	1	$6.06	
T-Slotted Framing 1 ft: T-Slotted Framing, Single Four Slot Rail, Silver, 1" High x 1" Wide, Solid, 1 ft	McMaster-Carr	47065T101-47065T411	$8.670	2	$17.34	
T-Slotted Framing 1 1/2 ft: T-Slotted Framing, Single Four Slot Rail, Silver, 1" High x 1" Wide, Solid, 1 1/2 ft	McMaster-Carr	47065T101-47065T554	$10.240	1	$10.24	
Propeller DAL 5045	Hobby Wireless	Product SKU: 3743-27	$0.990	1	$0.99	12V 17.6A 687g/ decided not to order this
Propeller: APC5x3E	APC	LP05030E	$2.550	1	$2.55	17.5V 12.9A 620g
Propeller: APC6x3R	APC	LP06030R-RH	$3.350	1	$3.35	17.6V 9.4A 489g

Future Work

We will run the motor in velocity or PWM modes so that the number of revolutions is not limited. Ideally, there should be no large resistance when detaching suction cups. To detach reliably, we need to develop a mechanism that breaks the cup seal by deforming or letting air in.

We could potentially use a small cam, wedge, or lever to flex the cup lip and break the seal, or peel off the cup with a wire.

Additionally, we hope to traverse curved surfaces better by having slack at the bottom of the belt so that the tread can conform to and take the shape of a curve. This may involve a simple linear actuator to tighten and loosen the belt. Once basic locomotion is achieved, we will begin work on a steering mechanism. Our idea is to use two extendable arms that can attach to the surface, lift the GelBelt off the structure, rotate it, and then reattach it so the robot can continue moving in a new direction. In the future, we have also discussed possibly integrating with some quadrotor design, which could make the platform even more mobile and assist with steering.